Supplementary Information (SI) for Journal of Materials Chemistry A.

Supporting Information

Photosynthesis-Inspired Dual-Mode Self-Healing Coatings: Leveraging Peony-like ZnO for Corrosion Interception and Energy Harvesting

Yinxia Dong [a], Libo Tong [a, *], Xiangjun Li [a], Miaomiao Li [a], Wenting Liu [a], Rongtao Wu [a], Xinyu Wang [a], Shiwei Xu [b], Kuaishe Wang [a]

[a] School of Metallurgical Engineering, Xi'an University of Architecture and Technology, Xi'an 710055, China

[b] State Key Laboratory of Advanced Design and Manufacturing for Vehicle Body, Hunan University, Changsha 410082, China

[*] Corresponding author.

E-mail addresses: lbtong@xauat.edu.cn (L. Tong).

Fax: 86-029-82202227

Adhesion test

The adhesion tests employ the crosscut method, with the standardized experimental procedure as follows: First, select an area free of blemishes or minor surface imperfections, ensuring the coating surface is smooth and free of impurities. Use a scalpel to cut a 6×6 grid pattern (each square measuring 4 square millimeters) on the coating surface, ensuring the cut lines penetrate the coating to the substrate. After removing debris from the cut area, apply pressure-sensitive tape firmly to the grid surface and peel it off rapidly at a 180° angle. Adhesion grade is determined by observing the coating's peeling state within the grid area according to evaluation criteria. Each sample undergoes three repeated tests to minimize error.

Tribological test

The tribological test was conducted using an MS-T3001 rotating ball structure equipment (Lanzhou Huahui Instrument Technology Co., Ltd.). A 6 mm diameter steel ball was employed at a reciprocating speed of 150 rpm/min, with a rotational radius of 3 mm. A load of 1 N was applied, yielding a contact pressure of 654.83 MPa. The test was performed for 20 min under conditions of 25°C and 23% humidity.

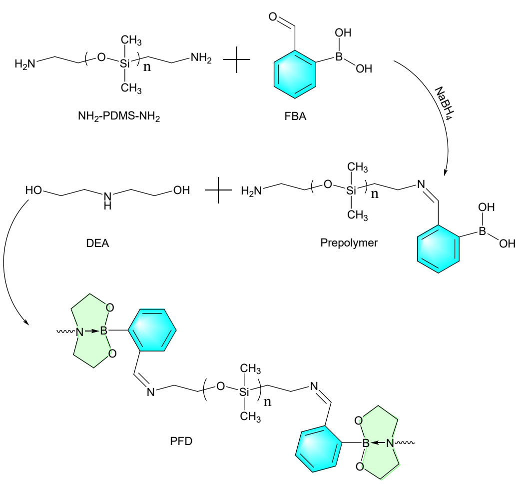

Fig. S1. Synthesis route of PFD.

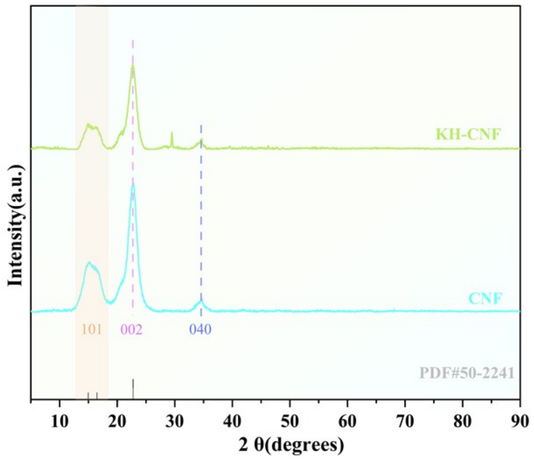

Fig. S2. XRD pattern of CNF and KMC.

The XRD patterns of CNF and KMCF reveal distinct crystallographic features. CNF exhibits characteristic diffraction peaks at 2θ = 14.98°, 16.48°, 22.78°, and 35°, corresponding to the (1**Error!**0), (110), (200), and (040) crystal planes, respectively [1].Modification with KH-550 preserves the fundamental crystal lattice of CNF, as evidenced by retained primary diffraction positions. However, reduced peak intensities indicate partial crystallinity loss attributable to amorphous silane side-chain grafting on CNF surfaces [2].

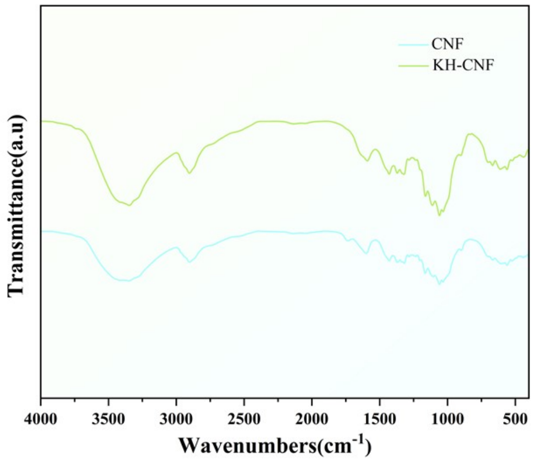

Fig. S3. FTIR spectra of CNF and KMC.

The structure of CNF and K-CNF was analyzed by FTIR (Fig. S3). Owing to the presence of the amino (-NH_2) and hydroxyl (-OH) functional groups in the coupling agent, the intensity of the broad absorption peak within the spectral curve of KMC, situated in the wavenumber range of 3000-3600 cm^{-1}, shows a noticeable increment. Furthermore, in the wavenumber range of 1000-1300 cm^{-1}, absorption peaks associated with the Si-O-Si bonds, which are formed as a result of the hydrolysis of KH-550, and the Si-O-CH_2 bonds, which are generated from the reaction between KH-550 and CNF, are expected to be present. Nevertheless, due to the fact that CNF displays intense absorption peaks in the identical region, it proves arduous to precisely ascertain the characteristic absorption peaks of Si-O-Si and Si-O-CH_3. Notwithstanding this, the intensity of the absorption peaks in this specific wavenumber range is remarkably augmented [3].

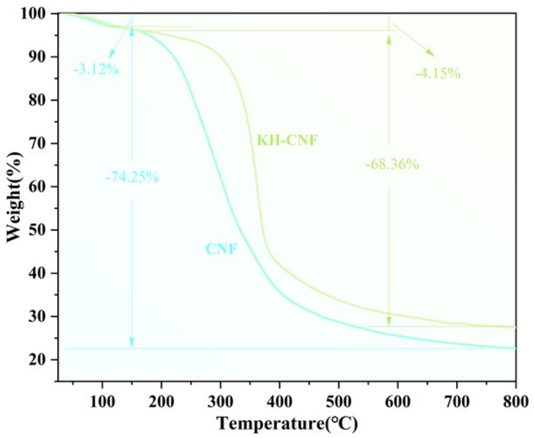

Fig. S4. TGA curves of CNF and KMC.

TGA was employed to assess the thermal stability of CNF and KMC. As evident from Fig. S5, both CNF and KMC exhibit two distinct weight loss stages. The first stage is attributed to the evaporation of moisture, resulting in weight losses of 3.12% and 4.15% for CNF and KMC, respectively. As the temperature rises, oxygen-containing functional groups commence degradation, and the carbon chain backbone begins to collapse or break, followed by carbonization [4]. Ultimately, CNF experiences a weight loss of 74.25% in the second stage. In contrast, due to the modification with KH-550, KMC shows a relatively lower weight loss of only 68.36%.

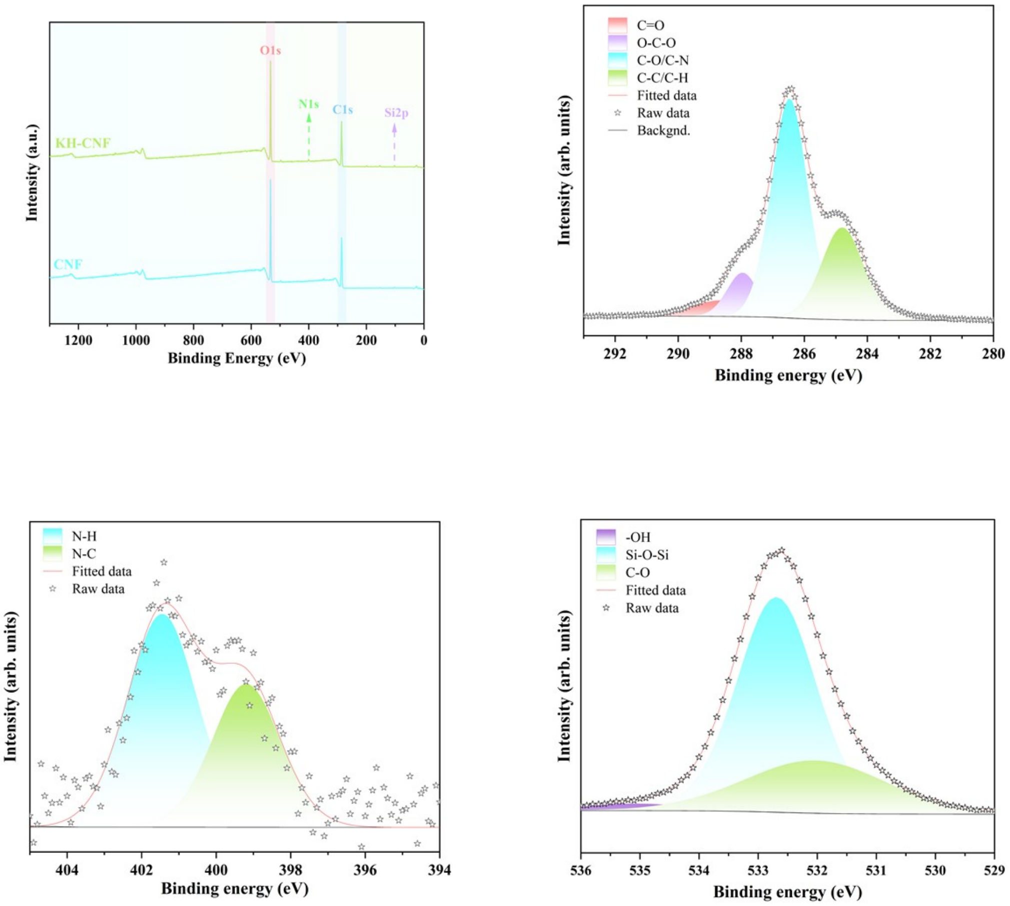

Fig. S5. High-resolution XPS spectrum of a) full spectra, b) C 1s, c) N 1s and d) O 1s. XPS was utilized to conduct further characterization of CNF and KMC. While both materials exhibit prominent C 1s and O 1s peaks, KMC demonstrates additional N 1s and Si 2p core-level signals. High-resolution analysis further identifies interfacial bonding configurations: the C 1s spectrum shows a characteristic C–N bond component at 284.8 eV, the N 1s spectrum displays a N–C coordination peak at 399.2 eV, and the O 1s spectrum reveals a Si–O bonding contribution at 532.7 eV. These collective observations validate covalent grafting of KH-550 onto the CNF surface through amine-hydroxyl interactions and siloxane network formation.

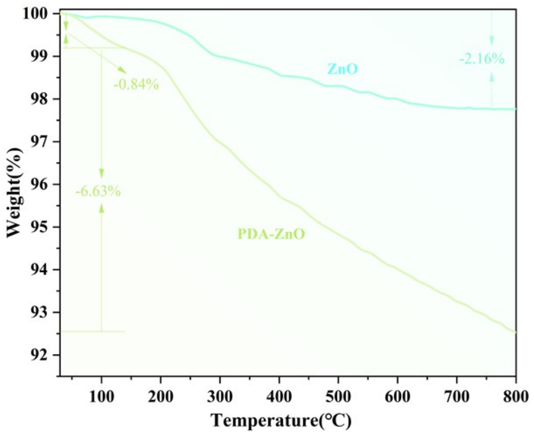

Fig. S6. TGA curves of ZnO and PFZ.

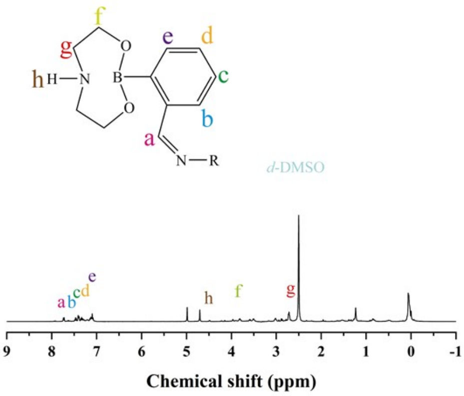

Fig. S7. 1H NMR spectrum for PFD in DMSO.

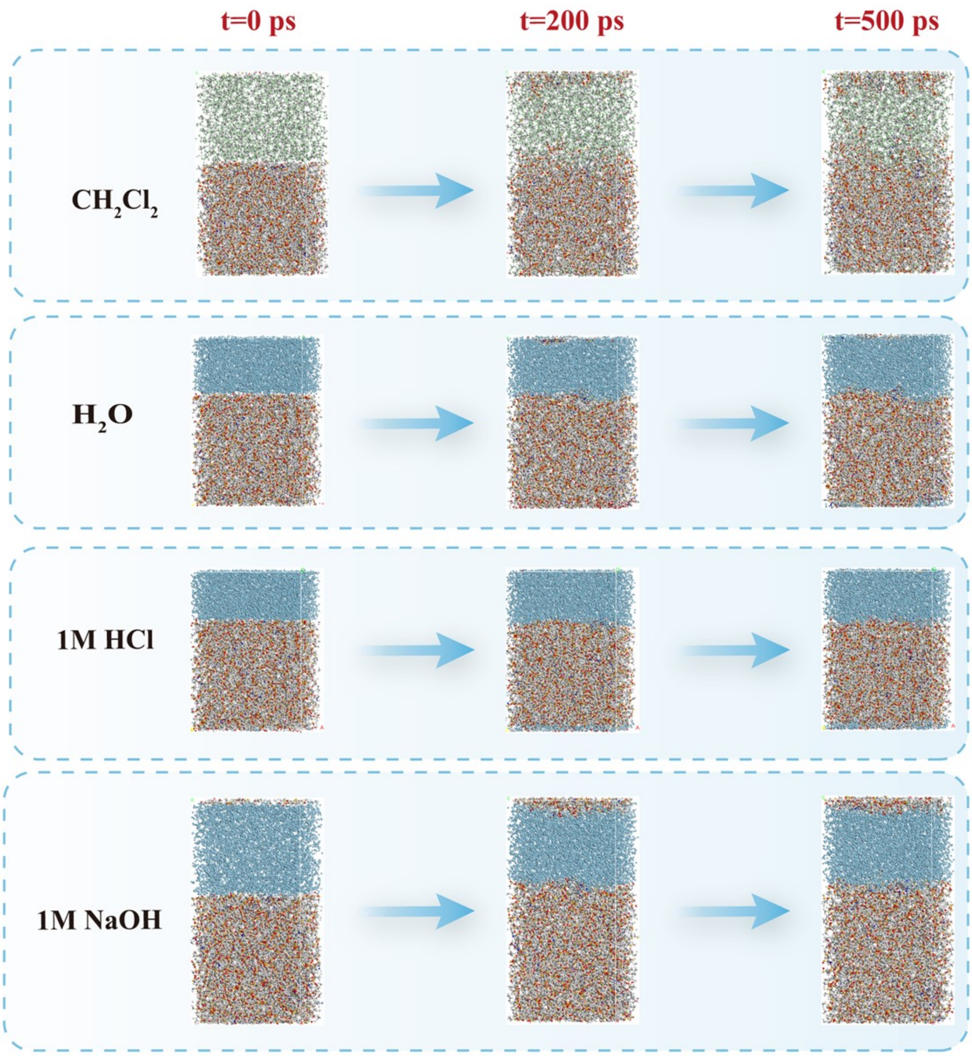

Fig. S8. Stability simulations of PFD in a) CH_2Cl_2, b) H_2O, c) 1M HCl solution and d) 1M NaOH solution.

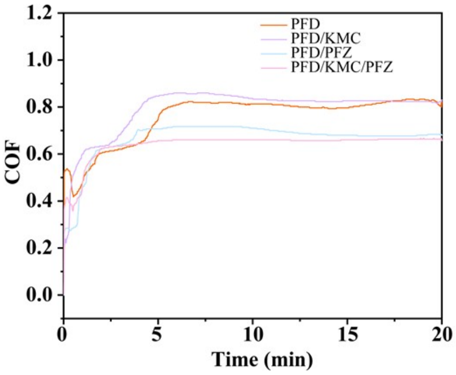

Fig. S9. COF curves for PFD, PFD/KMC, PFD/PFZ and PFD/KMC/PFZ samples.

Table S1. Adhesion test results for different coatings

Sample	PFD	PFD/KMC	PFD/PFZ	PFD/KMC/PFZ
Adhesion Rating (0B-5B)	5B	5B	5B	5B
Macro-Image			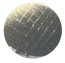	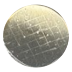

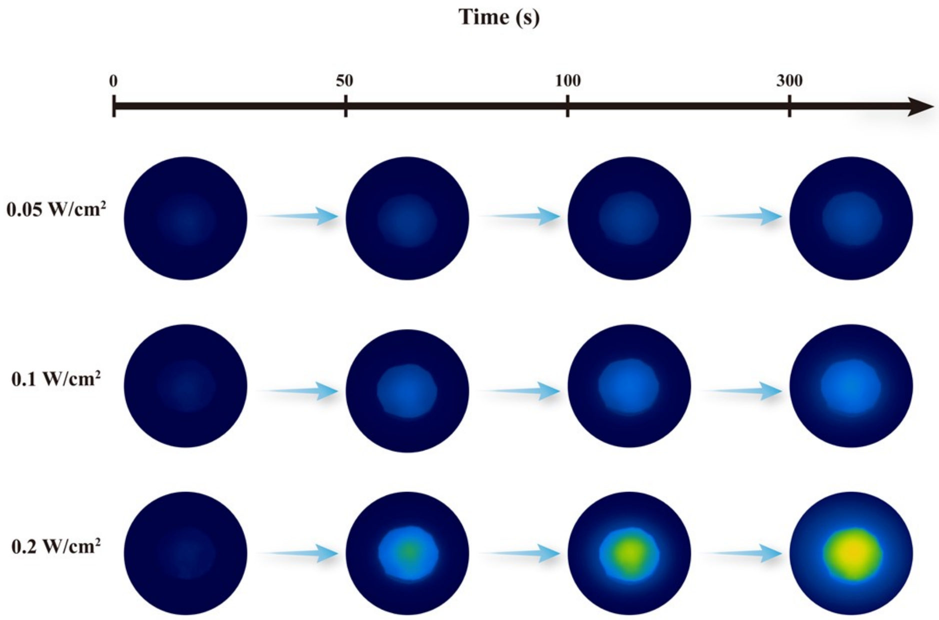

Fig. S10. Infrared thermography images of surface temperature changes of KMC/PFZ/PFD composite coatings under xenon lamp irradiation with different power densities (0.05 W/cm^2, 0.1 W/cm^2, and 0.2 W/cm^2).

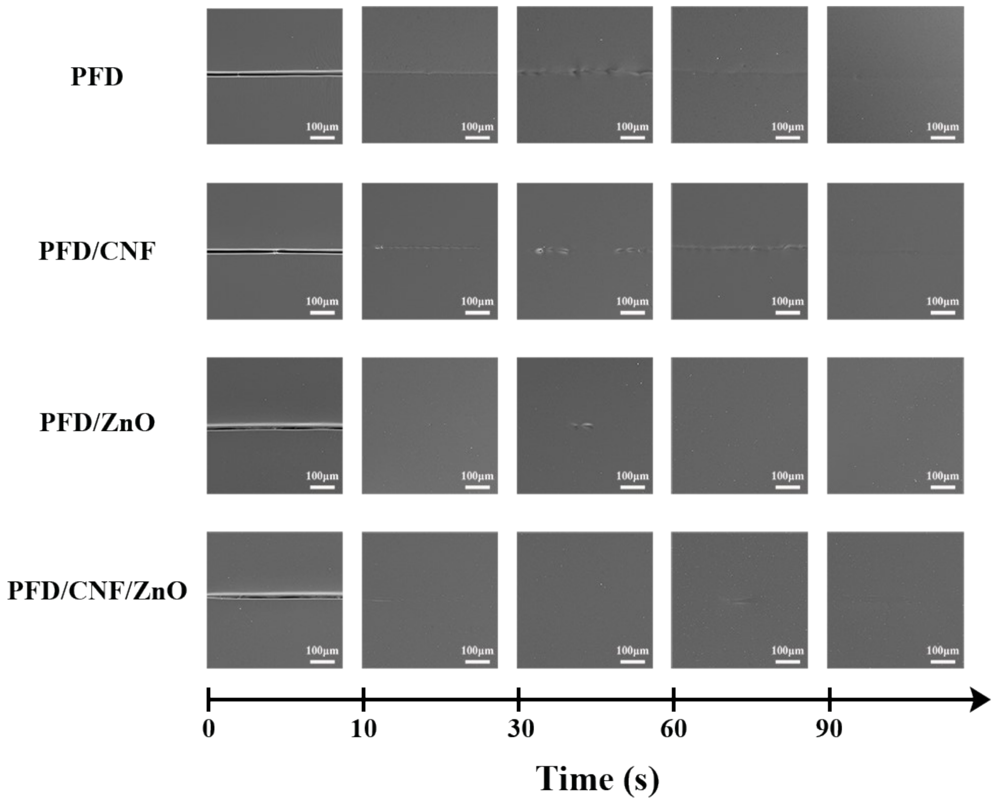

Fig. S11. SEM images of the natural healing process of scratches on coatings without xenon lamp irradiation (scale bar: 100μm).

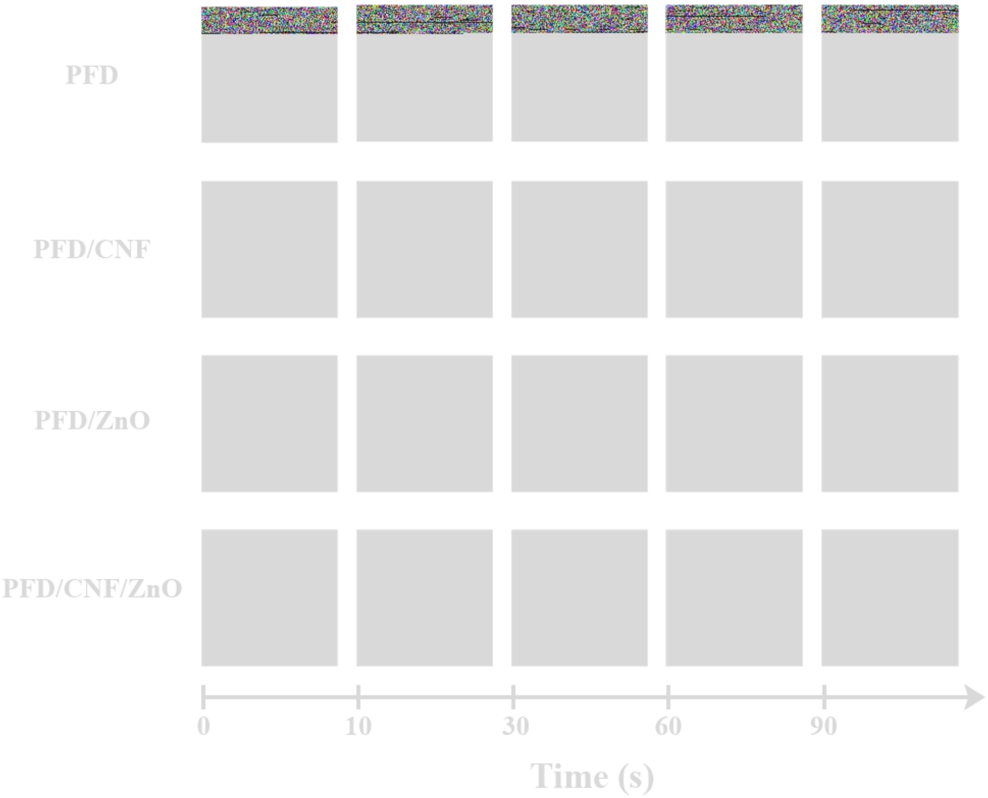

Fig. S12. SEM images of the self-healing process of scratches on coatings under xenon lamp irradiation at different times (scale bar: 100μm).

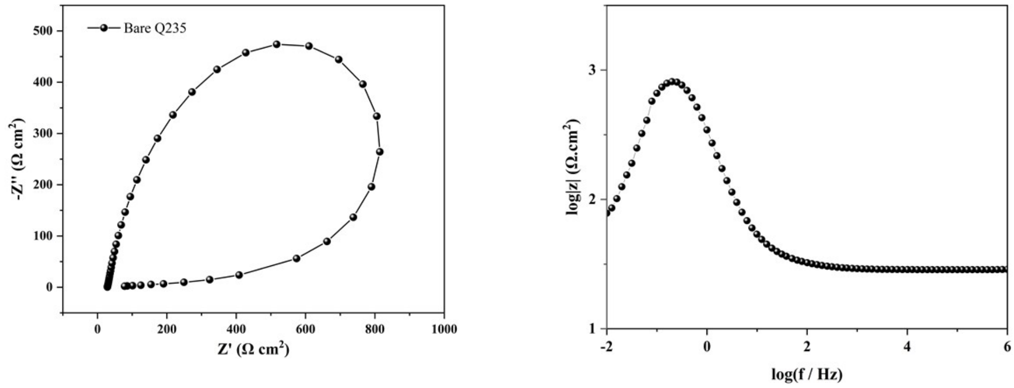

Fig. S13. a) Nyquist and b) Bode plot of bare Q235 steel substrate recorded after immersion in 3.5 wt.% NaCl solution for 0 h.

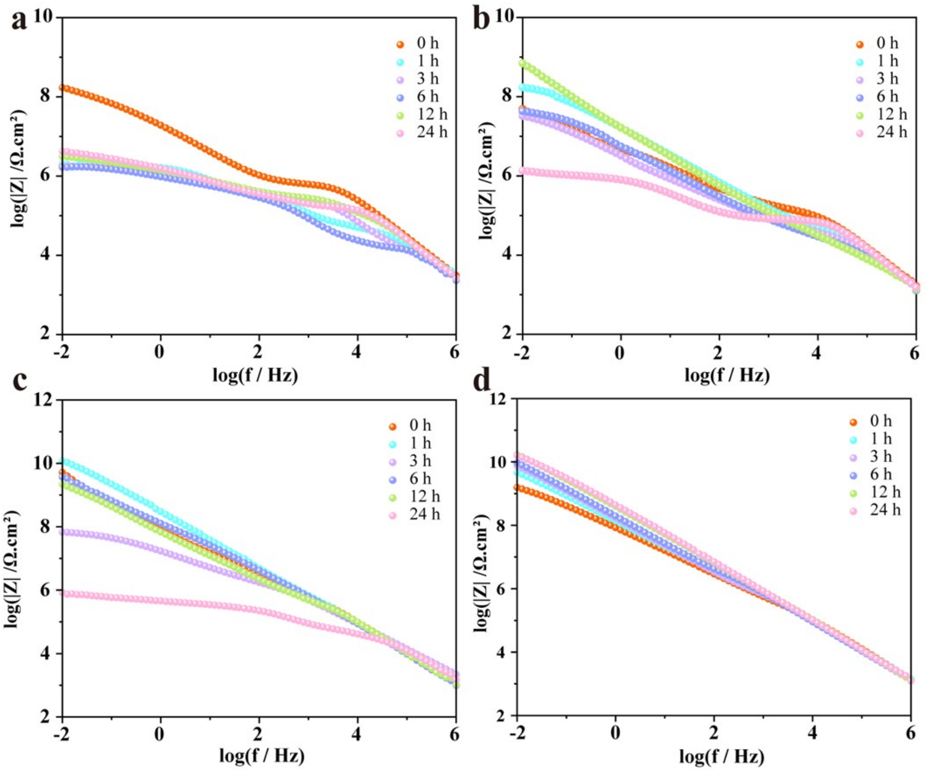

Fig. S14. The Bode plots of coatings obtained after immersion in 3.5wt.% NaCl for different times.

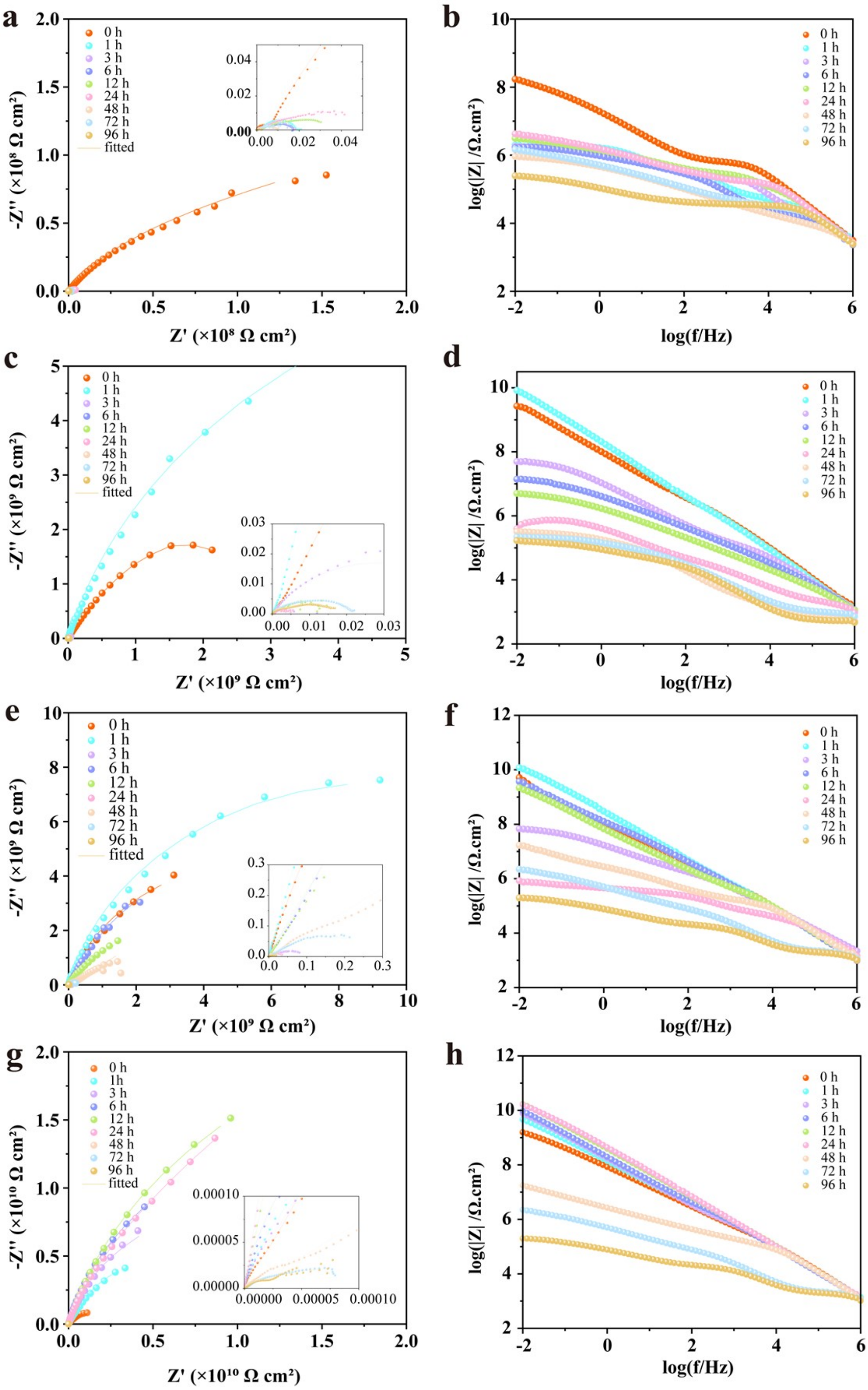

Fig. S15. Nyquist and Bode plots for coatings immersed in 3.5% wt.% NaCl solution for different times: a-b) PFD, c-d) PFD/KMC, e-f) PFD/PFZ and g-h) PFD/KMC/PFZ.

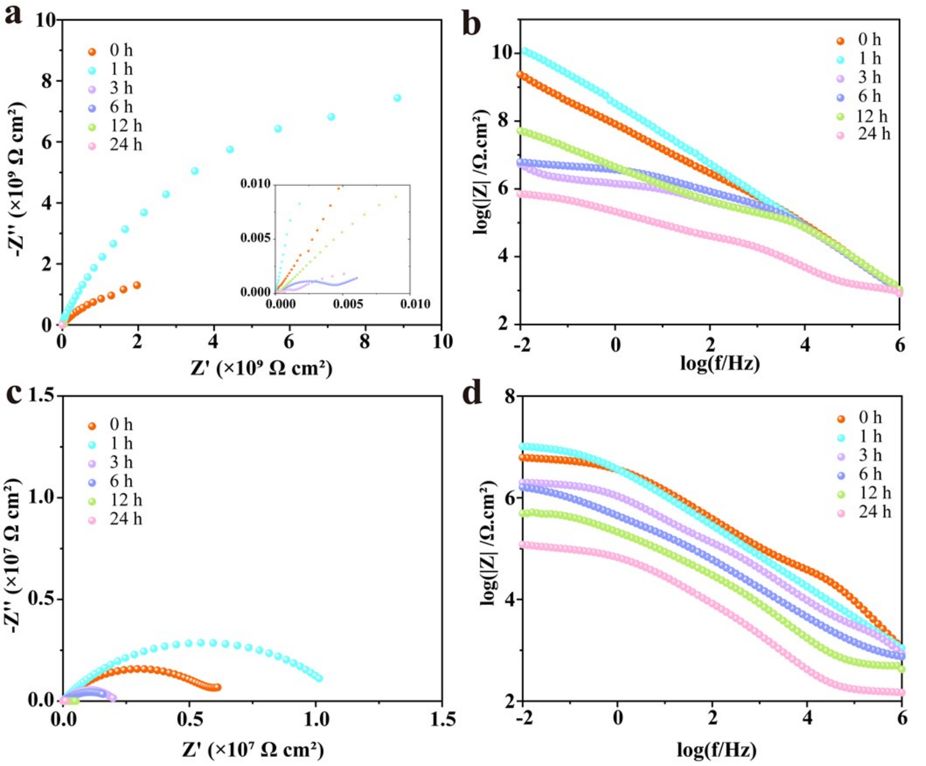

Fig. S16. Nyquist and Bode plots for coatings immersed in 3.5% wt.% NaCl solution for different times: a-b) PFD/KMC/spherical ZnO, c-d) PFD/KMC/nanorod ZnO.

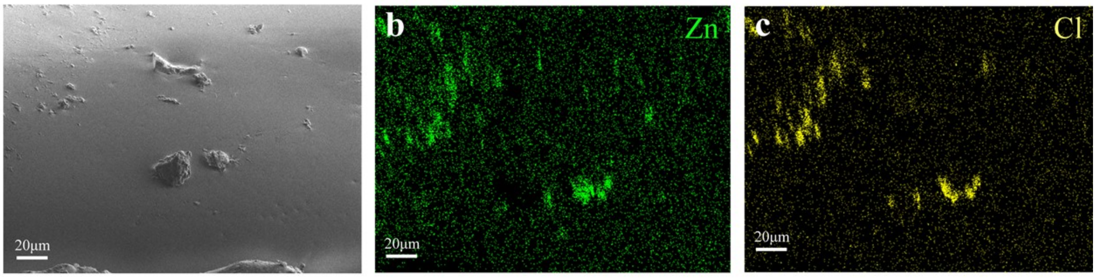

Fig. S17. SEM image and elemental mapping of the cross-section after corrosion of the PFD/KMC/PFZ.

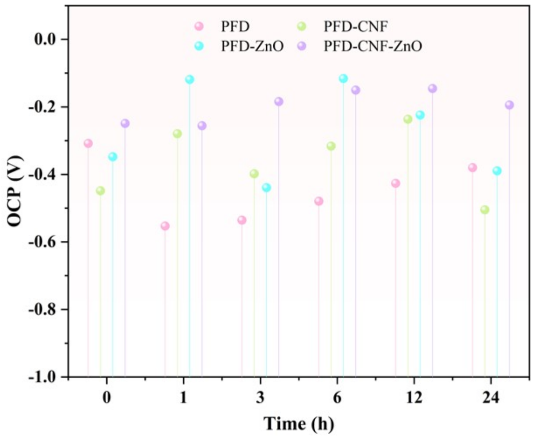

Fig. S18. OCP values of coatings.

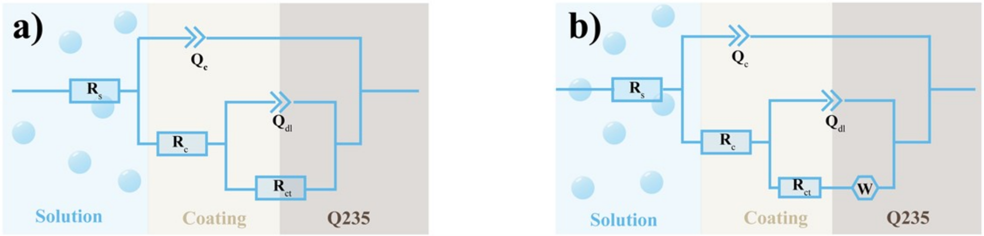

Fig. S19. The EEC models used for fitting the EIS data of different coatings, where R_s, R_c, and R_{ct} represented solution resistance, coating resistance, and charge transfer resistance, respectively. The constant-phase elements Q_c and Q_{dl} represent the capacitive response of the coating and bilayer, while the Warburg element (W) indicates increased cathodic corrosion. a) represents cases where the electrolyte reached steel substrate, while b) represents cases where the electrolyte reached the steel substrate, initiated the corrosion electrochemical reaction and generated corrosion products.

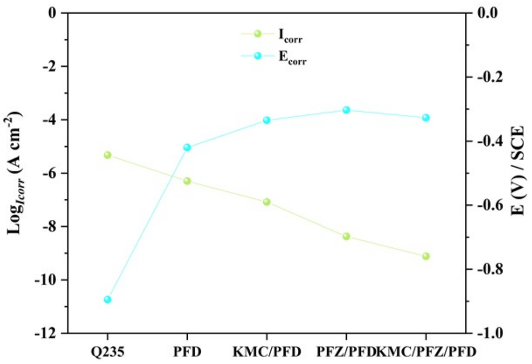

Fig. S20. Corrosion potential and corrosion current density of Q235 and coatings after 6 h of immersion tests.

Table S2. Parameters of polarization curves of coatings (1 cm^2) after 6 h immersion in 3.5wt.% NaCl solution obtained by Tafel extrapolation method.

Samples	I_{corr} (A cm^{-2})	E_{corr} (V)	β_c	β_a	CR (mm y^{-1})
Q235	4.786E-06	-0.895	-5.228	5.842	0.055
PFD	5.046E-07	-0.420	-0.134	0.393	0.005
PFD-CNF	8.245E-08	-0.335	-0.155	0.014	9.585E-04
PFD-ZnO	4.231E-09	-0.303	-0.112	0.429	4.918E-05
PFD-CNF-ZnO	7.655E-10	-0.327	-0.119	0.382	8.899E-06

The I_{corr}, E_{corr}, β_c, and β_a were processed by Tafel extrapolation, and the corrosion rate (CR) was calculated as the following equation [5]:

$$CR = (kM_m i_{corr})/n\rho_m$$

where k is a constant with a value of 3268.5 mol/A and M_m is the relative molar mass of the metal with the value of 55.845 g/mol. n is the number of charge transfers for the corrosion reaction of the metal and the value is 2. $\rho_m$is the density of the base metal and the value is 7.85 g cm^{-3}.

Table S3. Parameters of polarization curves of as prepared, scratched, and after healed coatings (1 cm^2) immersed in 3.5wt.% NaCl solution obtained by Tafel extrapolation method.

Samples	I_{corr} (A cm^{-2})	E_{corr} (V)	β_c	β_a
As prepared	8.610E-10	-0.293	-0.117	0.361
Scratched	9.270E-9	-0.381	-0.117	0.394
After healed	2.049E-9	-0.297	-0.129	0.336

Supporting References

1. Y. Zhang, X. Sun, Y. Ye, H. Oguzlu, Y. Zhu, J. Zhu, K. Le, P. Yang, F. Jiang, *Mater. Today*, **2024**, 74, 67-76.
2. K. Jin, Y. Tang, X. Zhu, Y. Zhou, *Int. J. Biol. Macromol.*, **2020**, 162, 1109-1117.
3. L. Huang, H. Zhao, T. Yi, M. Qi, H. Xu, Q. Mo, C. Huang, S. Wang, Y. Liu, *Nanomaterials*, **2020**, 10, 755.
4. X. Yang, Y. Jiang, R. Su, G. Yang, B. Xue, F. Li, *Colloids Surf., A*, **2016**, 509, 314-322.
5. Y. Huang, S. Yang, Y. Hu, H. Lin, J. Tang, C. Xu, Z. Yang, *Chem. Eng. J.*, **2024**, 487, 150539.